

## The Design of Planar Slot Arrays Revisited

J.C. Coetzee<sup>†</sup> and J. Joubert<sup>††</sup>

<sup>†</sup> Department of Electrical Engineering, National University of Singapore, 4 Engineering Drive 3, Singapore 117576

<sup>††</sup> Department Electrical & Electronic Engineering, University of Pretoria, Pretoria 0002, South Africa

### Abstract

Design procedures for planar waveguide slot arrays have been known and used for years, but the inexperienced designer is often faced with a number of practical problems when trying to implement them, especially in the case of larger arrays consisting of sub-arrays. Some helpful hints concerning the numerical implementation are provided. These include an effective procedure to avoid the necessity of good initial guesses for the unknown dimensions and recommendations for the subdivision of the nonlinear equations into smaller groups. Other practical aspects which are not explicitly defined elsewhere in the literature, are also addressed.

### 1. INTRODUCTION

Planar slot arrays are key components of high performance airborne radar systems, and also find application in modern microwave communication systems. A planar array consists of a number of slotted waveguides arranged side-by-side, while the most popular way of feeding the individual branches is through the use of crossed waveguide couplers with centred-inclined slots. For large arrays, the concept of sub-arraying is often used to improve the usable frequency bandwidth, and also to reduce the sensitivity of antenna performance on dimensional tolerances. Each sub-array is then fed by a main line, while the individual main lines are fed by a beam forming network. Slotted array seeker antennas also make use of sub-arraying, where a monopulse comparator network effectively feeds the four quadrants of the antenna either in-phase or out of phase with respect to each other.

Design procedures for the synthesis of linear slot arrays were proposed by Elliott [1-3], and were later extended to cover planar arrays [4]. Other contributions to the field of array design include those of [5] and [6]. Even though these techniques have been known and used for years, the inexperienced designer is still faced with a number of practical problems when trying to implement them, especially in the case of larger arrays consisting of sub-arrays. In this paper, some helpful hints concerning the numerical implementation are provided, and other practical aspects which are not explicitly defined elsewhere in the literature are addressed.

The design procedure involves the repeated solution of sets of nonlinear equations in order to iteratively compute the offsets and lengths of the radiating slots, as well as the inclination angles and lengths of coupling slots. The successful numerical solution of sets of nonlinear equations is usually dependent on the quality of the initial guesses for the unknowns, the number

of unknowns and also on the nature of the nonlinear equations. In practice, specifying suitable starting values may require considerable effort. In this paper, a simple but highly effective method, which is less dependent on good initial guesses and a priori knowledge about the eventual geometry, is proposed.

It is known that the solution obtained for a specific design is not unique, due to a number of degrees of freedom. This aspect is usually addressed by fixing some of the dimensions. A different way of accommodating the redundancy is proposed. It naturally divides the nonlinear equations into smaller groups by effectively decoupling them into semi-independent sets which are solved individually during each iteration.

There also seems to be some uncertainty regarding the correct orientation of coupling slots, especially when the array has more than one feed line. Unequivocal relations for the signs of radiating slot offsets and coupling slot angles are thus provided. Finally, some guidelines on the specifications for beam-forming networks required by multi-sub-array systems are given.

### 2. THEORETICAL BACKGROUND

Consider a planar array consisting of a total of  $S$  sub-arrays. The  $s$ th sub-array shown in Fig. 1 consists of a total of  $T_s$  branch lines, while the  $t$ th branch line has a total of  $N_{s,t}$  slots. The slots are resonantly spaced, i.e.  $d = \lambda_g/2$  and  $d_0 = \lambda_g/4$  at the design frequency,  $f_0$ . The inter-slot spacing should be larger than the waveguide width,  $a$ , and for a waveguide filled with a dielectric material of relative permittivity  $\epsilon_r$ , the value of  $a$  should be between the limits  $\lambda_0/2\sqrt{\epsilon_r} \leq a \leq \lambda_0/\sqrt{2\epsilon_r}$ , where  $\lambda_0$  is the free space wavelength. The thickness of the septum separating neighboring branches is thus  $t_0 = \lambda_g/2 - a$ . The waveguide height,  $b$ , may be chosen arbitrarily. The sub-array is fed by means of a main line, which is connected to the different branch lines via centred-inclined coupling slots. The coupling slot feeding the  $t$ th branch line of the  $s$ th sub-array has an inclination angle of  $\theta_{s,t}$ , and a slot length of  $l_{s,t}$ . The angle  $\theta_{s,t}$  is taken as positive in a clockwise direction. This coupling slot is located between the  $k_{s,t}$ th and the  $(k_{s,t}+1)$ th slot of the  $t$ th branch line. The term  $\hat{u}_s = u_s \hat{x}$  is the unit vector in the direction toward the shorted end of the main line, so that  $u_s = \pm 1$  for sub-arrays fed from the bottom and the top, respectively. The complete array has a total number of

$$M = \sum_{s=1}^S \sum_{t=1}^{T_s} N_{s,t} \text{ slots.}$$

Two distinct radiating slot indexing conventions are used:

- (a) A local numbering system with a triple index  $(s, t, n)$  denoting the  $n$ th slot in the  $t$ th branch line of the  $s$ th sub-array. The slot has a width of  $w$ , an offset of  $x_{s,t,n}^{\text{off}}$  relative to the center line of the branch line, and a slot length of  $L_{s,t,n}$ . Slots in a branch line are numbered from left to right, irrespective of whether the sub-array is fed from the bottom (as in Fig. 1) or from the top. Branch lines are numbered such that the line closest to the feeding end is denoted by  $t = 1$  and the line closest to the shorted end of the main line by  $t = T_s$ .
- (b) A global numbering system with a single index,  $i$ . The slot with local index  $(s, t, n)$  has a global index of

$$i = \sum_{u=1}^{s-1} \sum_{t=1}^{T_u} N_{u,t} + \sum_{v=1}^{t-1} N_{s,v} + n.$$

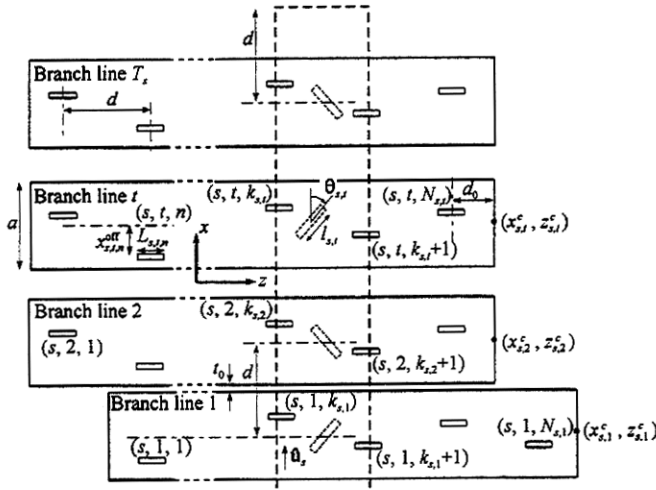


Fig. 1 Geometry of the  $s$ th sub-array.

The equivalent network for the  $n$ th branch line of the  $s$ th sub-array is shown in Fig. 2, where  $y_{s,t,n}^a$  is the normalized active admittance of the  $n$ th slot. The design procedure involves the repeated solution of a set of nonlinear equations in order to determine the slot offsets and lengths. The nonlinear equations are related to the so-called design equations, given by [2]

$$y_{s,t,n}^a = K_1 f_{s,t,n} \frac{V_{s,t,n}^{\text{slot}}}{V_{s,t,n}} \quad (1)$$

and [3]

$$\frac{1}{y_{s,t,n}^a} = \frac{1}{y_{s,t,n}^{\text{self}}} + \frac{1}{(f_{s,t,n})^2 K_2} \sum_{j=1, j \neq n}^M \frac{V_j^{\text{slot}}}{V_i^{\text{slot}}} g_{ji} + \frac{1}{(f_{s,t,n})^2 K_3} \left[ \frac{V_{s,t,n-1}^{\text{slot}}}{V_{s,t,n}^{\text{slot}}} h_{s,t,n} h_{s,t,n-1} + \frac{V_{s,t,n+1}^{\text{slot}}}{V_{s,t,n}^{\text{slot}}} h_{s,t,n} h_{s,t,n+1} \right] \quad (2)$$

For the slot with local index  $(s, t, n)$  and global index  $i$ , the slot voltage is denoted as  $V_{s,t,n}^{\text{slot}}$  or  $V_i^{\text{slot}}$ , while the corresponding

voltage in the equivalent network is  $V_{s,t,n}$ . The term  $y_{s,t,n}^{\text{self}} = y_{s,t,n}^{\text{self}}(x_{s,t,n}^{\text{off}}, L_{s,t,n})$  represents the normalized self-impedance of this slot. The function  $g_{ji}$  is given by [2], which is dependent on the coordinates of the centers of the  $i$ th and the  $j$ th slots. Let  $(x_i, z_i)$  the coordinates for the  $i$ th slot in the global coordinate system. In terms of the local coordinates, it is given by

$$(x_i, z_i) = (x_{s,t}^c + x_{s,t,n}^{\text{off}}, z_{s,t}^c - d_0 - N_{s,t}d + nd) \quad (3)$$

where  $(x_{s,t}^c, z_{s,t}^c)$  are the coordinates of the center point of the right edge of the  $n$ th branch line. The functions  $f_{s,t,n}$  and  $h_{s,t,n}$  may be obtained from [2] and [3] by making the substitutions  $2l_n = L_{s,t,n}$  and  $x_n = x_{s,t,n}^{\text{off}}$ . For  $n = 1$  or  $n = N_{s,t}$ , the undefined terms in (2) such as  $V_{s,t,0}^{\text{slot}}$ ,  $V_{s,t,N_{s,t}+1}^{\text{slot}}$ ,  $h_{s,t,0}$  and  $h_{s,t,N_{s,t}+1}$  may be found through the application of image theory. The constants  $K_1$ ,  $K_2$  and  $K_3$  may also be obtained from [2] and [3].

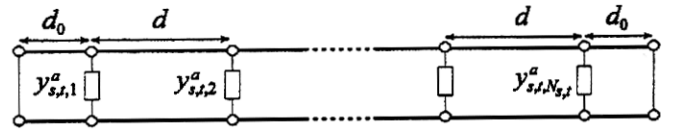


Fig. 2 Equivalent transmission line network for the  $n$ th branch line of the  $s$ th sub-array.

Let the voltages across the shunt elements in Fig. 2 be given by

$$V_{s,t,n} = q_{s,t} V_{s,t}^0 (-1)^{k_{s,t}-n} \quad (4)$$

The term  $q_{s,t}$  is an arbitrary constant equal to  $\pm 1$ , depending on whether the offset of the slot with index  $(s, t, k_{s,t})$  is to be positive or negative. These voltages are arbitrarily chosen to be real valued. Then  $V_{s,t}^0$  is a positive real number representing the magnitude of the voltages on the equivalent circuit of the  $n$ th branch line of sub-array  $s$ .

The series impedances of the equivalent circuit for the main line in Fig. 3 are given by [4]

$$z^{(s,t)} = (\kappa^{(s,t)})^2 y_{\text{in}}^{(s,t)} \quad (5)$$

where  $y_{\text{in}}^{(s,t)}$  is the normalized input admittance of the  $n$ th branch line of the  $s$ th sub-array, given by

$$y_{\text{in}}^{(s,t)} = \sum_{n=1}^{N_{s,t}} y_{s,t,n}^a \quad (6)$$

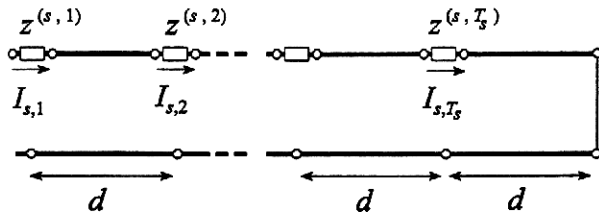


Fig. 3 Equivalent network for the main line of the  $s$ th sub-array.

The term  $\kappa^{(s,t)}$  is the coupling coefficient defined by

$$\kappa^{(s,t)} = \sqrt{\frac{S_{11}^{(s,t)}}{1 - S_{11}^{(s,t)}}} \quad (7)$$

while  $S_{11}^{(s,t)} = S_{11}(\theta = |\theta_{s,t}|, l = l_{s,t})$  is the scattering matrix component of the crossed waveguide couplers formed at the junction of the  $s$ th mainline and the  $t$ th branch line, as shown in Fig. 4. The normalized input impedance of the  $s$ th main line is then given by

$$z_{\text{in}}^{(s)} = \sum_{t=1}^{T_s} z^{(s,t)} = \sum_{t=1}^{T_s} (\kappa^{(s,t)})^2 y_{\text{in}}^{(s,t)} \quad (8)$$

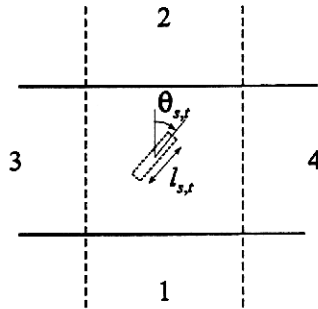


Fig. 4 Crossed-guide coupler geometry for the main line of the  $s$ th subarray and the  $t$ th stick.

Due to the fact that the coupling slots are also resonantly spaced (i.e.  $d = \lambda_g/2$  at the design frequency,  $f_0$ ), the current  $I_{s,t}$  in Fig. 3 is given by

$$\begin{aligned} I_{s,t} &= (-1)^{t-1} I_{s,1} \\ &= (-1)^{t-1} \frac{2a^{(s)}}{\sqrt{Z_0}(z_{\text{in}}^{(s)} + 1)} \end{aligned} \quad (9)$$

where  $I_{s,1}$  is the current at the first series element, while  $a^{(s)}$  is the incident wave intensity. Suppose the input impedance of each sub-array is purely resistive. Then  $z_{\text{in}}^{(s)} = r_{\text{in}}^{(s)}$ , where  $r_{\text{in}}^{(s)}$  is the chosen normalized input resistance of the  $s$ th sub-array as seen from the first series impedance in the main line equivalent circuit. The relation between the current at the

series impedance representing the  $t$ th coupling slot in the main line,  $I_{s,t}$ , and the voltage across the  $k_{s,t}$ th element in the equivalent network for the  $t$ th branch line,  $V_{s,t,k_{s,t}}$ , is given by

$$V_{s,t,k_{s,t}} = u_s \frac{\theta_{s,t}}{|\theta_{s,t}|} \kappa^{(s,t)} I_{s,t} \quad (10)$$

One design objective is to have all the slot voltages in phase. From equation (1), it follows that the argument of the term  $V_{s,t,k_{s,t}}/f_{s,t,n}$  should be uniform. In agreement with the choice of real-valued equivalent network voltages, this phase reference is taken to be zero. In a specific branch line, this is accomplished by alternating the offsets of the slots on opposite sides of the center line. The sign of the term  $f_{s,t,k_{s,t}}$  will be equal to the value of  $q_{s,t}$ , which implies that the sign of  $V_{s,t,k_{s,t}}$  should also be identical to the value of  $q_{s,t}$ . This agrees with the choice in (4). For resonant coupling slots,  $\kappa^{(s,t)}$  is purely real, while (9) and (10) dictate that  $a^{(s)}$  should also be real valued. Consequently, the orientations of the coupling slots are given by

$$\frac{\theta_{s,t}}{|\theta_{s,t}|} = (-1)^{t-1} u_s q_{s,t} \frac{a^{(s)}}{|a^{(s)}|} \quad (11)$$

Substituting (9) and (11) into (10) gives

$$V_{s,t,k_{s,t}} = q_{s,t} \kappa^{(s,t)} \frac{2|a^{(s)}|}{\sqrt{Z_0}(r_{\text{in}}^{(s)} + 1)} \quad (12)$$

A comparison of equations (4), (9) and (12) then yields the simple relation of [4], given by

$$V_{s,t}^0 = \kappa^{(s,t)} I_s^0 \quad (13)$$

where  $I_s^0 = |I_{s,t}|$ .

### 3. DERIVATION OF THE SETS OF NONLINEAR EQUATIONS

Consider the  $s$ th sub-array. Select the  $k_{s,t}$ th slot branch line  $t$  to serve as the reference slot. From equations (1) and (4), it is found that

$$\frac{y_{s,t,n}^a}{y_{s,t,k_{s,t}}^a} = \frac{f_{s,t,n} V_{s,t,n}^{\text{slot}} (-1)^{n-k_{s,t}}}{f_{s,t,k_{s,t}} V_{s,t,k_{s,t}}^{\text{slot}}} \quad (14)$$

Note that the ratio in (14) is only dependant on the slot offsets and lengths in branch line  $t$  of sub-array  $s$ . Equation (14) does not provide a sufficient number of equations to uniquely solve for the unknown slot offsets and lengths in the branch. It has been suggested that the slot which is to have the greatest slot offset be singled out and assigned an offset near the upper limit of reliable input data [4]. However, it is often difficult to identify this slot without some degree of a priori knowledge of the eventual geometry, especially in cases of uniform

excitation. A different approach is to specify the input admittance of each branch line to be purely real and with a normalized input admittance of  $g_{in}^{(s,t)}$ . Equations (6) and (14) may then be used to construct the following set of  $2N_{s,t}$  nonlinear equations for the unknown slot offsets and lengths of branch line  $t$  in sub-array  $s$ :

$$\text{Re} \left[ \frac{y_{s,t,n}^a}{y_{s,t,k_{s,t}}^a} - \frac{f_{s,t,n} V_{s,t,n}^{\text{slot}} (-1)^{n-k_{s,t}}}{f_{s,t,k_{s,t}} V_{s,t,k_{s,t}}^{\text{slot}}} \right] = 0$$

$$\text{Im} [y_{s,t,n}^a] = 0 \quad n = 1, 2, \dots, N_{s,t} \quad (15)$$

$$g_{in}^{(s,t)} - \text{Re} \left[ \sum_{n=1}^{N_{s,t}} y_{s,t,n}^a \right] = 0$$

where  $y_{s,t,n}^a$  is calculated using equation (2).

Comparing the active admittances of the  $k_{s,t}$ th slot of the  $t$ th branch line and the  $k_{s,1}$ th slot of the first branch line, using equations (1) and (12), results in

$$\frac{y_{s,t,k_{s,t}}^a}{y_{s,1,k_{s,1}}^a} = \frac{|f_{s,t,k_{s,t}}| V_{s,t,k_{s,t}}^{\text{slot}} \kappa^{(s,1)}}{|f_{s,1,k_{s,1}}| V_{s,1,k_{s,1}}^{\text{slot}} \kappa^{(s,t)}} \quad (16)$$

If the slot offsets and lengths of the reference slots are known, equations (8) and (16) may be used to construct the following set of  $2T_s$  nonlinear equations for the magnitude of the inclination angles and coupling slot lengths of main line  $s$ :

$$\text{Re} \left[ \frac{y_{s,t,k_{s,t}}^a}{y_{s,1,k_{s,1}}^a} - \frac{|f_{s,t,k_{s,t}}| V_{s,t,k_{s,t}}^{\text{slot}} \kappa^{(s,1)}}{|f_{s,1,k_{s,1}}| V_{s,1,k_{s,1}}^{\text{slot}} \kappa^{(s,t)}} \right] = 0 \quad t = 2, 3, \dots, T_s$$

$$\text{Im} [\kappa^{(s,t)}] = 0 \quad t = 1, 2, \dots, T_s \quad (17)$$

$$\text{Re} \left[ r_{in}^{(s)} - \sum_{t=1}^{T_s} (\kappa^{(s,t)})^2 g_{in}^{(s,t)} \right] = 0$$

where  $\kappa^{(s,t)}$  is calculated using (7).

#### 4. EFFECTIVE IMPLEMENTATION OF THE STARTING VALUE PROBLEM

Depending on the nature of a set of nonlinear equations, their numerical solution may be highly dependent on the quality of the initial guesses for the unknowns, as well as the number of unknowns. In the previous section, the equations were subdivided into smaller sets, but the designer is still faced with finding good starting values of the unknown slot dimensions.

For larger arrays, the evaluation of the external mutual coupling terms  $g_{ji}$  is generally the most time consuming step in the numerical implementation of a design procedure. For

practical purposes, an iterative approach for the design of linear arrays was proposed in [2], where during each iteration, these terms are computed using the current set of slot dimensions and are assumed to remain constant while calculating new dimensions by way of solving of a set of nonlinear equations. It was also suggested in [4] that the external and internal mutual coupling terms be set to zero for the first iteration. Due to the simplified nature of the resulting nonlinear equations, this negates the need for good initial guesses for the unknown as required by nonlinear equation solvers. Arbitrary starting values within the realistic range of slot dimensions may then be specified, while the nonlinear equation solver routine is usually successful in finding a solution. During the second iteration, the computed slot dimensions for the zero mutual coupling case are used to re-evaluate the mutual coupling terms, and the same dimensions are employed as starting values for the subsequent solution of the nonlinear equations. This approach is entirely effective for linear arrays. This is due to the fact that the mutual coupling between slots that are approximately axially aligned is relatively small, and therefore the abrupt inclusion of the mutual coupling contributions during the second iteration only has a secondary effect, and the changes in slot dimensions never become excessive.

For planar arrays the displacement between certain slots is also lateral, which causes the external mutual coupling to have a more pronounced effect on the slot dimensions. The examples in [3] bare evidence of this. Even though a uniform excitation for all slots was specified, the mutual coupling causes large variations in slot offsets, while in the absence of mutual coupling, all slots have the same lengths and offset magnitudes. Implementation of the approach proposed for linear arrays may result in numerical instability. Problems generally do not occur when solving for the zero mutual coupling case during the first iteration. However, during the second iteration where the zero mutual coupling dimensions (which may differ appreciably from the final results) are used to first calculate  $g_{ji}$  and then also as starting values for the subsequent solving of the nonlinear equations, the procedure often fails.

It is therefore proposed that the procedure be modified by retaining the first iteration with zero mutual coupling, but instead of abruptly introducing the effects of mutual coupling during the second iteration, that its effects be included gradually. This is achieved by weighing the values of  $g_{ji}$  and  $h_{s,t,n}$  with a weighting factor increasing from 0 to 1 during the first half of a chosen total number of iterations. Consequently, the first iteration will be performed with zero mutual coupling, while the full effect of the mutual coupling is only included during the second half of the iterations. This approach generously compensates for a possible increase in the total number of iterations by being very robust and reliable. The ease of implementation of this procedure is also an advantage

over other approaches which merely rely on good starting values that are obtained by for instance first considering an infinite array [6].

## 5. BEAM-FORMING NETWORK

An array consisting of a number of sub-arrays would naturally require a power splitter or beam-forming network to distribute the power from the antenna input to the multiple sub-array main lines. A complete design should therefore also include the specifications of the power splitter network. A comparison of the active admittances of the  $k_{s,1}$ th slot of the first branch line of sub-array  $s$  and of the  $k_{1,1}$ th slot of the first branch line of sub-array 1 using equations (1) and (12) yields the following relative amplitudes of the incident wave intensities for the sub-arrays:

$$\frac{|a^{(s)}|}{|a^{(1)}|} = \frac{|f_{s,1,k_{s,1}}| V_{s,1,k_{s,1}}^{\text{slot}} \kappa^{(1,1)} y_{1,1,k_{1,1}}^a (r_{\text{in}}^{(s)} + 1)}{|f_{1,1,k_{1,1}}| V_{1,1,k_{1,1}}^{\text{slot}} \kappa^{(s,1)} y_{s,1,k_{s,1}}^a (r_{\text{in}}^{(1)} + 1)} \quad (18)$$

The phase difference between  $a^{(s)}$  and  $a^{(1)}$  is either  $0^\circ$  or  $180^\circ$ . The phase relation is chosen in accordance with the phase properties of the beam-forming network to be used. Together with (18), the ratio  $a^{(s)}/a^{(1)}$  is thus completely specified. In general, an array consisting of  $S$  sub-arrays would require a splitter with  $P = S + 1$  ports. For the sake of clarity, it is assumed that each of the first  $S$  ports is connected to its corresponding sub-array, while the  $P$ th port serves as the common feed port. From the definition of the scattering parameters, it follows that

$$[S^{\text{split}}] [a^{\text{split}}] = [b^{\text{split}}] \quad (19)$$

$[S^{\text{split}}]$  is the  $P \times P$  scattering parameter matrix of the network, specified with the phase reference of port 1 to port  $S$  at the center of the first coupling slot of the main line it is connected to. Since the first  $S$  ports of the splitter network are terminated in the input impedances of the sub-arrays, it follows that

$$a_s^{\text{split}} = \Gamma_{\text{in}}^{(s)} b_s^{\text{split}} \quad s = 1, 2, \dots, S \quad (20)$$

where

$$\Gamma_{\text{in}}^{(s)} = \frac{r_{\text{in}}^{(s)} - 1}{r_{\text{in}}^{(s)} + 1} \quad (21)$$

The wave emanating from the  $s$ th port is fed directly into the main line of the  $s$ th sub-array, while the antenna should normally be matched at port  $P$ . This implies that

$$b_s^{\text{split}} = \begin{cases} a^{(s)} & s = 1, 2, \dots, S \\ 0 & s = P \end{cases} \quad (22)$$

For a lossless splitter network, the conservation of power condition requires that

$$\sum_{s=1}^P (|a_s^{\text{split}}|^2 - |b_s^{\text{split}}|^2) = 0 \quad (23)$$

Using (22) and (23) together with the specification for  $a^{(s)}/a^{(1)}$  then gives

$$\frac{b_s^{\text{split}}}{a_p^{\text{split}}} = \begin{cases} \frac{\frac{a^{(s)}}{a^{(1)}} e^{j\zeta}}{\sqrt{\sum_{m=1}^S \left(\frac{a^{(m)}}{a^{(1)}}\right)^2 [1 - \Gamma_{\text{in}}^{(m)2}]}}, & s = 1, 2, \dots, S \\ 0 & s = P \end{cases} \quad (24)$$

$\zeta$  is an arbitrary common phase term. The relations in (24) specify the requirements for the splitter network. The simplest way of realizing this would be to design the sub-arrays to be matched (i.e.  $r_{\text{in}}^{(s)} = 1$  and  $\Gamma_{\text{in}}^{(s)} = 0$ ), which would then require that

$$S_{sP}^{\text{split}} = \begin{cases} \frac{(a^{(s)}/a^{(1)}) e^{j\zeta}}{\sqrt{\sum_{m=1}^S (a^{(m)}/a^{(1)})^2}} & s = 1, 2, \dots, S \\ 0 & s = P \end{cases} \quad (25)$$

## 6. DESIGN PROCEDURE

Array design requires data on the self admittance of isolated radiating slots as a function of the slot offset and length, as well as scattering parameters for coupling slots in terms of the inclination angle and slot length. These may either be obtained through measurement or calculation. In the case of the latter, the formulations in [7] and [8] may be used to pre compute the databases, while a bivariate spline interpolation scheme as in [9] has proved to be very effective for the calculation of the terms  $y_{s,t,n}^{\text{self}} = y^{\text{self}}(x_{s,t,n}^{\text{off}}, L_{s,t,n})$  and  $\kappa^{(s,t)} = \kappa(|\theta_{s,t}|, l_{s,t})$ . The design procedure then consists of the following:

1. Specify the slot voltages  $V_{s,t,n}^{\text{slot}}$  for a desired radiation pattern.
2. Specify  $u_s$  for each sub-array, as well as  $q_{s,t}$  and  $k_{s,t}$  for each branch line.
3. Select realistic values for the input conductance of each branch line,  $g_{\text{in}}^{(s,t)}$ . A guideline is to choose a typical slot offset  $x_{\text{typ}}^{\text{off}}$  and to identify the corresponding resonant length for this offset,  $L_{\text{typ}}$ . A typical value for the input conductance would then be  $g_{\text{in}}^{(s,t)} = N_{s,t} \cdot y^{\text{self}}(x_{\text{typ}}^{\text{off}}, L_{\text{typ}})$ .
4. Specify the input resistance of each main line,  $r_{\text{in}}^{(s)}$ . Unless the circumstances dictate otherwise, the most convenient choice would be  $r_{\text{in}}^{(s)} = 1$ .
5. Select an appropriate number of iterations to be performed,  $C$ , where  $C \geq 10$  is an even-valued integer.
6. Select initial guesses for the lengths and offsets for the

- radiating slots. An effective choice is to select  $x_{s,t,n}^{\text{off}} = (-1)^{k_{s,t}-n} q_{s,t} x_{\text{typ}}^{\text{off}}$  and  $L_{s,t,n} = L_{\text{typ}}$ .
7. Select initial guesses for the magnitude of the inclination angles and slot lengths for the coupling slots.
  8. Set the iteration counter  $c = 1$ .
  9. Calculate the global slot coordinates using equation (3).
  10. Calculate the mutual coupling terms  $g_{ji}$  and  $h_{s,t,n}$ .
  11. For the first half of the total number of iterations ( $c < C/2$ ), weigh the values of  $g_{ji}$  and  $h_{s,t,n}$  with a factor of  $2(c-1)/C$ , i.e. scale all the elements of  $g_{ji}$  to  $2(c-1)g_{ji}/C$  and the elements of  $h_{s,t,n}$  to  $2(c-1)h_{s,t,n}/C$ .
  12. Set  $s = 1$ .
  13. Set  $t = 1$ .
  14. Solve the set of  $2N_{s,t}$  nonlinear equations in (15) for the unknown slot offsets and lengths of branch line  $t$  in sub-array  $s$ :  $(x_{s,t,n}^{\text{off}}, L_{s,t,n})$  where  $n = 1, 2, \dots, N_{s,t}$ .
  15. Increment  $t$  and repeat step 14 until  $t = T_s$ .
  16. Solve the set of  $2T_s$  nonlinear equations in (17) for the magnitude of the inclination angles and coupling slot lengths in main line  $s$ :  $(|\theta_{s,t}|, l_{s,t})$  where  $t = 1, 2, \dots, T_s$ .
  17. Increment  $s$  and repeat steps 13-16 until  $s = S$ .
  18. Increment  $c$  and repeat steps 9-17 until  $c = C$ .
  19. Calculate the ratios of the wave intensities that a power splitter network needs to supply to the different sub-arrays from (18).
  20. Specify the phase relation at each of the first  $S$  ports of the power splitter, i.e. whether sub-arrays are to be fed in phase or  $180^\circ$  out of phase relative to the excitation of the first sub-array, and use (11) to determine the orientation of the coupling slots.

## 7. DESIGN EXAMPLE

As an example, a small array similar to the one shown in Fig. 5 was designed. It consists of four sub-arrays, each having three branches and three slots per branch. A design frequency of  $f_0 = 9$  GHz was chosen, and half-height X-band waveguide of width  $a = 22.86$  mm and height  $b = 5.08$  mm was used for the branch guides and feed lines. A database for the properties of isolated radiating slots and inclined coupling slots was computed, using a slot width of  $w = 1.5875$  mm and a waveguide wall thickness of  $t = 1.27$  mm. A uniform excitation for all radiators was adopted. The array was designed to have a normalized conductance of  $g_{\text{in}}^{(s,t)} = 1.5$  for all branches, and a normalized input resistance of  $r_{\text{in}}^{(s)} = 1$  for each of the four sub-arrays. From the geometry, it follows that  $u_1 = u_2 = -1$ ,  $u_3 = u_4 = 1$ ,  $k_{1,t} = k_{4,t} = 1$ ,  $k_{2,t} = k_{3,t} = 2$  and  $q_{s,t} = -1$ . A total number of ten iterative steps were used during the design. The computed slot offsets and slot lengths for the radiating slots are shown in Table I, while the inclination angles and lengths of the coupling slots are listed in Table II. Due to the symmetry, sub-arrays 1 and 3 and sub-arrays 2 and 4 are mirror images of each other, and therefore corresponding slots will have the same magnitude of offset or

inclination angle, but with a difference in sign.

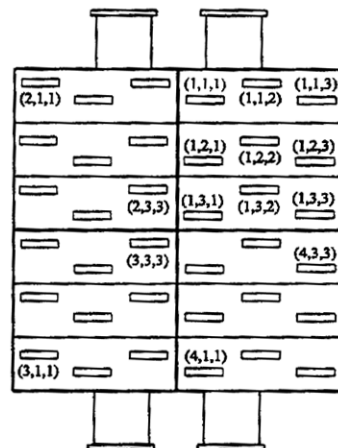


Fig. 5 Geometry of a  $4 \times 3 \times 3$  array.

Table I Slot offsets and slot lengths of radiating slots.

Slot index $(s, t, n)$	$x_{s,t,n}^{\text{off}}$ (mm)	$L_{s,t,n}$ (mm)
(1,1,1), (3,1,3)	$\mp 2.256$	16.758
(1,1,2), (3,1,2)	$\pm 3.015$	16.821
(1,1,3), (3,1,1)	$\mp 2.397$	16.779
(1,2,1), (3,2,3)	$\mp 2.859$	16.822
(1,2,2), (3,2,2)	$\pm 1.958$	16.287
(1,2,3), (3,2,1)	$\mp 2.221$	16.574
(1,3,1), (3,3,3)	$\mp 2.177$	16.842
(1,3,2), (3,3,2)	$\pm 1.516$	16.787
(1,3,3), (3,3,1)	$\mp 2.325$	16.830
(2,1,1), (4,1,3)	$\pm 2.848$	16.828
(2,1,2), (4,1,2)	$\mp 2.012$	16.630
(2,1,3), (4,1,1)	$\pm 3.138$	16.923
(2,2,1), (4,2,3)	$\pm 1.976$	16.437
(2,2,2), (4,2,2)	$\mp 2.679$	16.610
(2,2,3), (4,2,1)	$\pm 2.153$	16.500
(2,3,1), (4,3,3)	$\pm 1.969$	16.888
(2,3,2), (4,3,2)	$\mp 2.188$	16.756
(2,3,3), (4,3,1)	$\pm 1.603$	16.885

Table II Inclination angles and slot lengths of coupling slots.

Slot index $(s, t)$	$\theta_{s,t}$ (degrees)	$l_{s,t}$ (mm)
(1,1), (3,1)	$\pm 23.61$	16.986
(1,2), (3,2)	$\mp 21.47$	16.970
(1,3), (3,3)	$\pm 18.58$	16.948
(2,1), (4,1)	$\pm 24.73$	16.998
(2,2), (4,2)	$\mp 20.81$	16.964
(2,3), (4,3)	$\pm 17.88$	16.943



Due to the symmetry, the incident wave intensities were found to be  $a^{(s)}/a^{(1)} = 1$  for all sub-arrays.

The effect of the gradual inclusion of the mutual coupling is illustrated in Fig. 6, where the variation of the offset for the slot with index (1,3,2) as computed during the iterative steps is shown. The initial offset calculated for the case with zero mutual coupling is 3.082 mm, while the final offset is only 1.516 mm. The gradual introduction of the mutual coupling contributions over the next five iterative steps avoids abrupt changes in the slot dimensions, and convergence is easily achieved during the second half of the iterations.

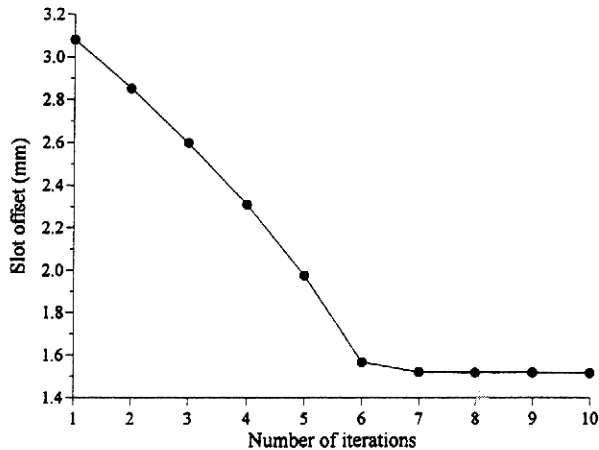


Fig. 6 Offset of slot (1,3,2) as computed during each iterative step.

## 8. CONCLUSION

The repeated computation of the external mutual coupling between slots, which involves numerical integration, is the most time-consuming part of the procedure. Utilization of an alternative expression for the coupling coefficient [10] results in an appreciable increase in efficiency. Some numerical experimentation may be required in order to obtain a design where all the slot offsets are within the desirable range. Slot offsets of less than  $w/2$  should be avoided. Care should also be taken not to allow the offsets to become too large, especially when using waveguides of reduced height. This may lead to problems related to the validity of the equivalent circuit models for the slots [11]. If the computed offsets of a particular branch are either too large or too small, the input conductance of those branches should be decreased or increased and the design repeated. Used in conjunction with an analysis procedure [12], the admittance levels of the branch lines may be chosen so as to optimize the off-centre frequency performance of the array.

The proposed algorithm is easily translated into computer code, and has been applied successfully to the design of arrays of varying sizes. The process of subdividing the nonlinear equations into smaller groups and gradually introducing the

effects of mutual coupling has proven to be very reliable when used in conjunction with reliable nonlinear equation solver routines.

## REFERENCES

- [1] R.S. Elliott and L.A. Kurtz, "The Design of Small Slot Arrays", *IEEE Trans. Antennas Propagat.*, vol. AP-26, no. 3, pp. 214-219, Mar. 1978
- [2] R.S. Elliott, "An Improved Design Procedure for Small Arrays of Shunt Slots", *IEEE Trans. Antennas Propagat.*, vol. AP-31, no. 1, pp. 48-53, Jan. 1983.
- [3] R.S. Elliott, "The Design of Slot Arrays Including Internal Mutual Coupling", *IEEE Trans. Antennas Propagat.*, vol. AP-34, no. 9, pp. 1149-1154, Sept. 1986.
- [4] R.S. Elliott, "The Design of Waveguide-Fed Slot Arrays", in Y.T. Lo and S.W. Lee (Edits.), *Antenna Handbook*, Van Nostrand Reinhold, 1988.
- [5] A.J. Angster and A.H.I. McCormick, "Theoretical design and synthesis of slotted waveguide arrays", *IEE Proc. H Microwaves, Antenna & Propag.*, vol. 136, no. 1, pp. 39-46, Feb. 1989.
- [6] H. Y. Yee, "The Design of Large Waveguide Arrays of Shunt Slots", *IEEE Trans. Antennas Propagat.*, vol. 40, no. 7, pp. 775-781, July 1992.
- [7] L.G. Josefson, "Analysis of Longitudinal Slots in Rectangular Waveguides", *IEEE Trans. Antennas Propagat.*, Vol. AP-35, pp. 1351-1357, Dec. 1987.
- [8] W. Hanyang and W. Wei, "Moment method analysis of a feeding system in a slotted-waveguide antenna", *IEE Proc. H Microwaves, Antenna & Propag.*, Vol. 135, pp. 313-318, Oct. 1988.
- [9] D.A. McNamara and J. Joubert, "On The Use of Bivariate Spline Interpolation of Slot Data in the Design of Slotted Waveguide Arrays", *ACES J.*, vol. 9, no. 1, pp. 6-9, 1994.
- [10] G. Mazzarella and G. Panariello, "Fast computation of mutual coupling in slot arrays", *Microwave J.*, pp. 193-196, June 1988.
- [11] G.J. Stern and R.S. Elliott, "Resonant Length of Longitudinal Slots and Validity of Circuit Representation: Theory and Experiment", *IEEE Trans. Antennas Propagat.*, vol. AP-33, no. 11, pp. 1264-1271, Nov. 1985
- [12] J.C. Coetzee, J. Joubert and D.A. McNamara, "Off-Center-Frequency Analysis of a Complete Planar Slotted Waveguide Array Consisting of Sub-Arrays", submitted for publication in *IEEE Trans. Antennas Propagat.*